970–981 Vol. 78 No. 4 ACTA GEOLOGICA SINICA Aug. 2004
http://www.geojournals.cn/dzxbcn/ch/index.aspx

Textural and Geochemical Characteristics of Proglacial Sediments: A Case Study in the Foreland of the Nelson Ice Cap, Antarctica

LIU Xiaodong, SUN Liguang and YIN Xuebin
Institute of Polar Environment, University of Science and Technology of China, Hefei, Anhui 230026; E-mail: ycx@ ustc.edu.cn or slg@ustc.edu.cn

Abstract This paper presents a detailed study on the textural and geochemical characteristics of the proglacial sediments near the edge of modern Nelson Ice Cap, Antarctica. The grain size distributions of the proglacial sediments are characteristic of glacigenic deposits, but very different from those of aeolian and lacustrine sediments. Moreover, the grain size distributions of the proglacial sediments are fractal with a dimension of about 2.9, and the fractal dimensions can be used as another summary statistical parameter for quantifying the relative amounts of coarse and fine materials. Correlations between the absolute element abundances of the proglacial sediments are very weak due to mineral partitioning and other effects of glacial processes, but correlations between the element/Rb ratios are statistically significant. This finding indicates that element/Rb ratios can be used to reduce or eliminate the effects of glacial processes, evaluate geochemical data and determine the sediment provenance in the foreland of Antarctic glacier. Comparisons on the element concentrations among different environments suggest that the proglacial sediments are derived predominantly from local bedrocks and appear to be natural in origin. Thus these natural sediments can be used to study chemical weathering in the proglacial foreland of modern glacier.

Key words: proglacial sediment, grain size, fractal dimension, element abundance, chemical weathering

1 Introduction

Parts of the Antarctic Ice Sheet have fluctuated substantially during the Quaternary, although its overall configuration has been stable for the past 14 million years (Ingólfsson et al., 1998). The retreat of glacier ice exposes a landscape susceptible to nonglacial conditions. The modification, caused by glaciation-conditioned nonglacial processes, has been termed paraglaciation by Church and Ryder (1972). It refers both to proglacial processes and those occurring around and within the margin of a former glacier, such as mass movement processes, frost action processes, fluvial processes, aeolian processes (Fitzsimons, 1996; Ballantyne, 2002).

Antarctic glaciation produces a large amount of detrital material in the form of glacial drift, and the widespread paraglacial reworking of glacial drift after ice retreat ultimately results in redeployment of such sediments in new settings. In the past 12 years, there has been a remarkable flourishing of researches and publications devoted to paraglacial processes, paraglacial sediment transport and paraglacial landscape modification (Ballantyne, 2002). Of these publications, only a few are about Antarctic paraglacial deposits. And these studies are focused on observations of periglacial geomorpholoy, analysis of paraglacial sedimentary processes and descriptions of weathering processes (Fitzsimons, 1990, 1996; Matsuoka et al., 1990, 1992, 1995; Lundqvist et al., 1995; French and Guglielmin, 1999). Concerning the nature of paraglacial sediments themselves, such as textural and geochemical characteristics, however, little information is available. This may be due to the fact that the formation of these reworked glacigenic sediments is a highly complex process (Jari, 1995; Klossen, 1999).

In this study, the proglacial sediment cores from the margin of Nelson Ice Cap on the Nelson Island, west Antarctica, are selected to study their textural and geochemical characteristics. Our main objectives are to (1) examine their grain size distributions, (2) investigate a suitable approach for processing their geochemical data, and (3) quantitatively evaluate the degree of chemical weathering of silicate materials on the glacial foreland.

2 Study Area

The Nelson Island (62°14′–62°21′ S, 59°14′–58°49′ W) is situated on the southwestern side of the King George Island, the largest one among the South Shetland Islands, and is about 500 m southwest to the east coast of the Fildes Peninsula (Fig. 1). This island has a north-south span of 12 km and an east-west span of 18 km. Among a total surface area of about 164.8 km^2, approximately 95% of the island is covered with ice and snow, and the exposed area is only

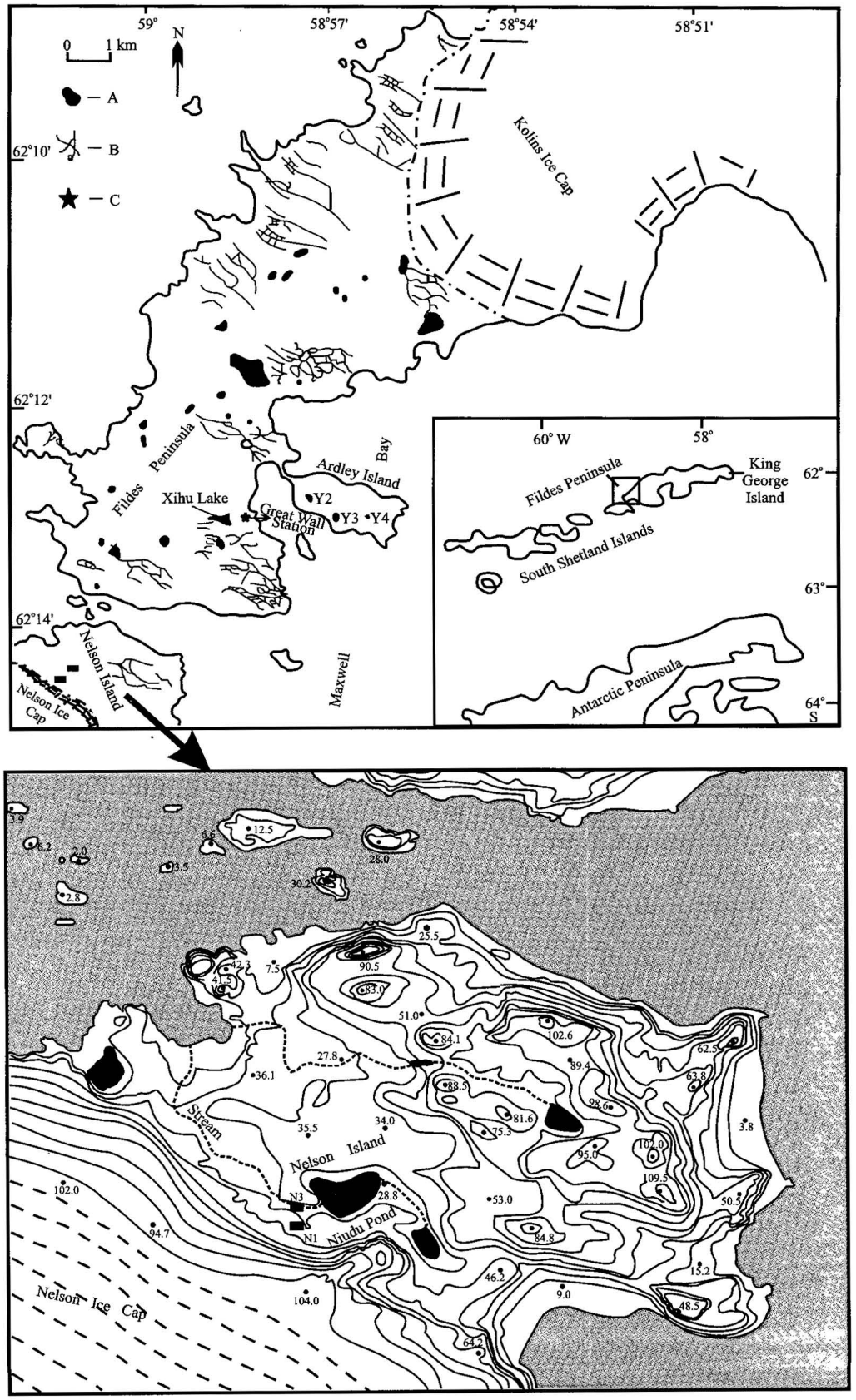

Fig. 1. The study area and sampling sites for N1, N3, Y2, Y3 and Y4.
Upper: A – lake; B – network of meltwater channels; C – the Great Wall Station.

about 8.5 km^2. The Nelson Ice Cap is a "warm" and thin glacier due to the strong influence of the sub-Antarctic maritime climate (Rin et al., 1995). The outcropping bedrock in the ice-free area is dominated by Tertiary basaltic and andesitic lavas, approximately the same as that on the adjacent Fildes Peninsula (Zhen et al., 2000). The bare bedrock is sparsely vegetated by lichens, algae and mosses.

The Nelson Island has an oceanic climate, typical of maritime Antarctica, with frequent summer rains and a moderate annual thermal amplitude. According to the meteorological records from the Great Wall Station, which is located on the Fildes Peninsula and about 3 km northeast from the studied site, the mean annual precipitation is about 630 mm, and the average annual relative humidity is about 90%. The mean annual air temperature is around –2.6°C, with a winter low at –26.6°C, summer high at 11.7°C and a summer (December to March) average temperature above 0°C. This climate results in the freeze-thaw cycles and an active layer. The melt-water from ice and snow appears to be the primary control on the type and rate of depositional processes. The depositional processes in the ice-marginal area, dominated by mass washing of debris-mantled rock slopes, transportation of surface debris and transport of debris in small seasonal streams, take place during the short summer period. Most debris in the ice-free area of Nelson Island consists of the paraglacially reworked glacigenic sediments, and some may be from weathering due to the frequent diurnal freeze-thaw cycles in summer. The glacial origin of these materials is discernible from the meltout, glacially striated boulders, and a grain size distribution of poor sorting (discussed below). Several cold monomictic ponds are formed throughout the ice-free area of the Nelson Island in bedrock depressions and are generally ice-free during January and February. The pond water is fed by meltwater from snow drift, ice and local precipitation; it is sterile and nutrient-deficient. The sediments in these small and shallow ponds are mostly coarse to fine sand, primarily a kind of glaciofuvial deposit.

3 Samples and Methods

The sediment cores N1 and N3 were collected from the northern ice-free area of the Nelson Island about 50 m and 70 m from the front margin of the Nelson Ice Cap, respectively (Fig. 1). N1 is located at the foot of a detris-mantled slope with a gradient of about 30°. The down-slope movement of debris at this site, as described by Fitzsimons (1990, 1996), is apparently initiated through saturation by meltwater from snow and ice during the short summer. The unconsolidated deposits in N1 is mainly derived from slope-washing sediments. N3 is close to the Niudu pond (Fig. 1), where short seasonal stream drains melting snow and ice into the pond, so this pond acts like a sediment trap. The sediments in N3 have undergone reworking by glaciofluvial surface-washing processes. The sediment cores N1 and N3 are 66 cm and 73 cm long, respectively. For the purpose of comparison, aeolian and lacustrine sediments were also collected. A 52 cm-long aeolian sediment sequence (as marked by Y3 in Fig. 1) was taken from the margin of a wind-facing slope on the Ardley Island (Sun et al., 2002). Two lake sediment cores Y2 and Y4 of 67.5 cm and 34 cm long, respectively, were collected from the Ardley Island (Fig. 1). We used PVC plastic gravity pipes of 12 cm diameter to drill down to the bedrock, and extruded vertically to collect these sediment samples.

Grain size distribution analyses were performed at 2 cm intervals for the proglacial and aeolian sediment cores. In addition, we also used the grain size composition analysis results of 332 subsamples from the lacustrine sediment samples taken from the present Xihu Lake near the Chinese Great Wall Station (unpublished data from a research report on the China Ninth Five-Year project of tackling key problems). Chemical element analyses were performed for sediment cores N1 and Y4 at 2 cm intervals. For Y2, a total of 24 subsamples at an appropriate interval were analyzed by Sun et al. (2001).

The water and organic contents in these subsamples are determined according to the procedure by Heiri et al. (2001). Subsamples of the wet sediment from N1 were analyzed for water content by drying for 24 h at 105°C, and the dried samples were then ashed for a further 3 h at 550°C to determine the percent loss on ignition (LOI).

For grain size distribution analysis, each weighted sample was firstly sieved through a 500-μm sieve. A model SALD-3001 laser particle analyzer was used to record the grain size composition of the fractions with diameters less than 500 μm. All the results were recalculated for bulk samples. The grain size compositions and the statistical parameters, including mean grain size (Mz), mean square deviation (σ), skewness (Ski) and kurtosis (Kg), were calculated according to Folk and Ward (1957). To determine whether the grain size distributions of the proglacial sediments are fractal, we presented size distribution data in terms of the number of particles within a given size range according to Hooke and Iverson (1995) and compared each other as bivariate plots of log number of particles against log particle diameter.

For chemical element analysis, subsamples from N1, Y2 and Y4 were ground to a 200-mesh size after drying in open air. About 0.1–0.5 g of each powder sample was taken, precisely weighed, and then digested by with the HF-HNO_3-$HClO_4$ mixed solution in a Pt crucible with electric

heating. The digested samples were analyzed for the following 22 elements: Na, K, Ca, Mg, Mn, Fe, Ti, Al, Si, Zn, Cu, Ge, Ni, As, S, F, Rb, Sr, Ba, Cr, P and V. Concentrations of SiO_2, Al_2O_3 and Fe_2O_3 were determined by various wet chemical methods. S was analyzed by the KI volume method after combustion in an SRJK-2 high-temperature furnace. F was measured by the ion selective electrode (ISZ). Trace elements Sr and Ba were determined using the inductively coupled plasma-atomic emission spectrometry (ICP-AES) after digestion by aqua regia/HF/$HClO_4$, and the instrument used was the Atom Scan Advantage. Abundances of P_2O_5, TiO_2, Cr, V and B were determined by ultraviolet visible spectrophotometry (UVS). Concentrations of As were determined by atomic fluorescent hydrogenation (AFS) (XDY-1 atomic fluorescent spectrometry). Atomic absorption spectrophotometry (AAS) (Model PZ-1100) was used to determine K_2O, Na_2O, CaO, MgO, MnO, Ni, Cu, Zn and Ga. For determination of CaO in silicate phase only, carbonate bearing samples were treated with 1M cold dilute HCl acid before digestion. For calculation of the chemical index of alteration (CIA), P_2O_5-corrected CaO concentration in the silicate phase was used (Sharma and Rajamani, 2000, 2001). The precision and accuracy of our results were monitored using reference samples in every batch of analyses. The measured values of the reference samples were in good agreement with the reference values, the differences being within ±5%.

4 Results and discussion

4.1 Textural characteristics

Grain size distribution of sedimentary materials is widely utilized to glean information about sedimentary processes and environments (Liu et al., 2001; Li et al., 2002). The grain size distribution data of N1 and N3 are given in Table 1 and Fig. 2. As seen from the figure and table, the grain sizes in N1 and N3 show wide-ranging distributions. For N1, the portion of clay-size material varies from 6.79% to 18.79%, that of silt from 17.78% to 53.17%, that of sand from 9.60% to 29.15% and that of gravel from 6.90% to 60.87%. Primarily due to the reworking by meltwater, N3 is enriched in sand-sized particles, slightly deficient in gravel, silt and clay as compared to N1. The overall grain size parameters of N1 are similar to those of N3 (Table 1). Their mean grain size is of the sand grade, with extremely poor sorting, positive skewness and broad to medium kurtosis. The grain size compositions for the reworked proglacial sediments N1 and N3 are very different from those for aeolian and lacustrine sediments. The proglacial sediments consist largely of gravel and show poor sorting, but the aeolian and lacustrine sediments consist mostly of sorted sand or silt plus clay (Table 1). In addition, the water content in N1 is quite low (<20%) and quite evenly distributed, reflecting good compaction throughout the profile. The LOI values are also very low (<5%) and change little down core, reflecting a low organic content (shown in Fig. 2). These are characteristic of glacigenic sediments.

The method by Hooke and Iverson (1995) was used to test whether the grain size distribution of a sediment sample is fractal. This method has been used for analyzing the particle number versus size distribution, and the deforming subglacial tills were found to be fractal, reflecting scale-invariant debris comminution processes (Hooke and Iverson, 1995; Iverson and Hooyer, 1996; Fischer and Hubbard, 1999; Khatwa et al., 1999). This method, however, has not been applied to the proglacial sediments. Figure 3 is the typical bivariate plots of grain diameter versus number of particles for one representative sample from the N1 and N3 profiles. The least square fitting gives a correlation coefficient larger than 0.98, a good indication of fractal distributions. Based on all best-fit lines, we found that the grain size distributions of sediments in N1 and N3

Table 1 Grain-size distributions for proglacial sediments (N1, N3), aeolian sediments (Y3), and present Xihu Lake sediments (XH)

Sample		Gravel (%) (>2 mm)	Sand (%) (2 mm–63 μm)	Silt (%) (63–2 μm)	Clay (%) (<2 μm)	Mz (ϕ)	σ (ϕ)	Ski	Kg
N1 (n=35)	Range	6.90–60.87	9.60–29.15	17.78–53.17	6.79–18.79	0.45–5.80	3.93–5.18	0.18–0.76	0.60–1.39
	Average	34.03	19.36	34.43	12.18	2.77	4.70	0.20	0.70
N3 (n=39)	Range	0.73–62.23	10.18–73.12	5.53–70.16	2.27–16.43	–0.77–6.2	2.35–4.78	0.20–0.83	0.71–3.57
	Average	18.09	46.27	27.39	8.26	2.48	3.59	0.40	1.21
Y3 (n=27)	Range	0	67.97–99.91	0.023–27.08	0–13.65	1.64–4.08	0.23–3.05	0.14–0.84	0.80–5.40
	Average	0	85.28	9.71	5.01	2.83	1.57	0.46	2.10
XH (n=332)[a]	Range	0	0.013–80.25	22.53–87.13	3.30–31.65	3.37–7.14	1.35–2.50	0.076–2.19	2.06–7.11
	Average	0	8.00	71.55	20.61	6.34	1.90	0.61	2.76

Note: The data with superscrip "a" are from Yuan et al. (personal communication, 2000).

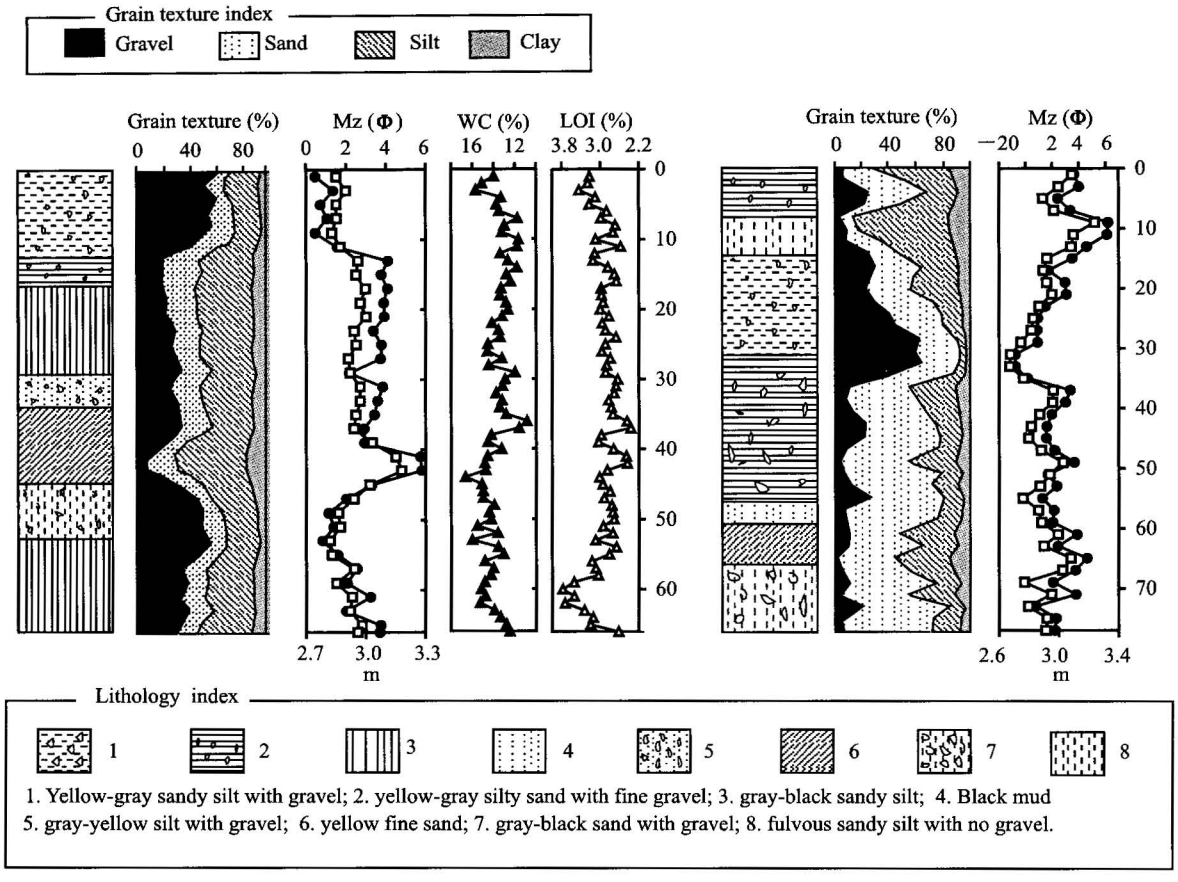

Fig. 2. Vertical variations of grain texture, mean grain size (Mz), fractal dimensions (m), water content (WC) and loss of ignition (LOI) in the proglacial sediments N1 and N3.

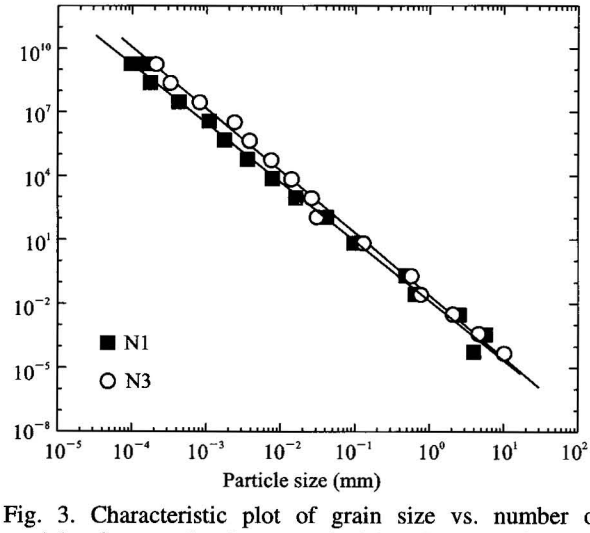

Fig. 3. Characteristic plot of grain size vs. number of particles for samples from proglacial sediments. The solid rectangles and hollow circles represent the typical particle size distributions for the N1 and N3 profiles, respectively.

were fractal distributions, and their inferred fractal dimensions, as calculated as the slopes of least square fitting, were from 2.82 to 3.18 with a mean of 2.92 and from 2.67 to 3.24 with a mean of 2.84, respectively. The above mean fractal dimensions are very close to 2.90, as reported by Hooke and Iverson (1995) and Khatwa et al. (1999) for deformed glacial sediments, 1 that these re-deposited sediments in the periglacial foreland have inherited the signal of grain size distributions from the glacial tills. Indeed, the deformed glacigenic materials are the main material source of the proglacial sediments at the margin of the Nelson Ice Cap. Figure 2 illustrates the relationship between the fractal dimensions and grain size data within the stratigraphic cores N1 and N3. It can be observed that the fractal dimension values (m) are inversely correlated with the proportion of coarse materials, but positively correlated with the fine materials and the average grain size (Mz). Consequently, the fractal dimensions of proglacial sediments, as suggested by Benn and Gemmell (2002) using the method of numeral simulations, are likely related to the relative amounts of coarse and fine materials in the distribution, indicating that mechanical mixing of parent materials by paraglaciation may take place in the formative process of the proglacial sediments near modern glacier. Thus the fractal dimensions of naturally occurring proglacial sediments can be used as another summary statistical parameter for grain size distribution. A further

research suggests that the fractal dimensions of samples from the foreland of modern Nelson Ice Cap have significant environmental implications. They are the integrated results of the glacial dynamic process, sedimentary environment and paleoclimatic evolution. According to the variable trend of the fractal dimensions, we could reconstruct the evolutionary history of paleoclimatic environment and ice sheet advance and retreat in this area (Liu et al., 2003).

4.2 Geochemical characteristics

Table 2 gives the arithmetic mean, variable range and coefficient of variation (CV) for the chemical concentration of elements in N1. For comparative purposes, the average element concentrations in local bedrocks, lacustrine sediments (Y2 and Y4) and Xihu Lake sediments are also given in this table. As seen from the table, the mean element concentrations in N1 are similar to those in the local bedrocks, but significantly different from those in the

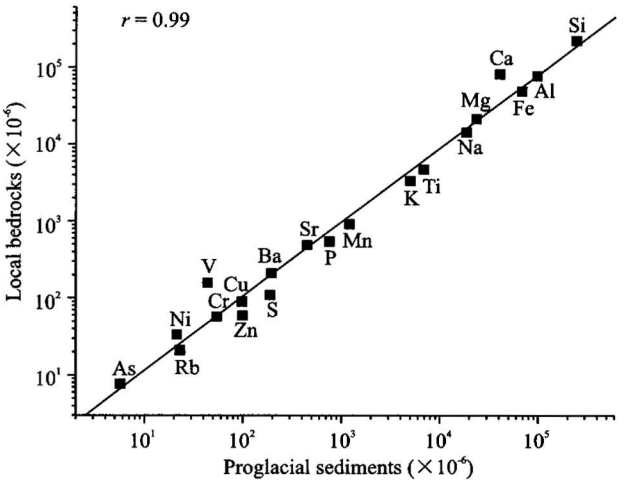

Fig. 4. Comparison of average element concentrations between the proglacial sediment N1 and local bedrocks. The correlative coefficient is greater than 0.99, indicating a good agreement between the two.

Table 2 Chemical element concentrations in proglacial sediments (N1), local bedrocks and lake sediments (Y2, Y4 and Xihu Lake)

	Profile N1 (n=35)			Bedrock (n=51)[a]	Y4 (n=19)	Y2 (n=24)[b]	Xihu (n=26)[c]
	Range	CV (%)	Mean	Mean	Mean	Mean	Mean
				Major elements (%)			
Na	1.64–2.01	5	1.84	1.47	1.08	1.86	1.84
K	0.38–0.61	10	0.50	0.34	0.27	0.54	0.47
Ca	3.38–4.55	6	3.99	8.48	11.95	7.68	2.88
Mg	2.09–2.93	4	2.31	2.20	0.73	1.38	1.43
Mn	0.098–0.18	12	0.12	0.093	0.12	0.073	0.078
Fe	6.10–7.47	9	6.71	5.07	5.71	5.02	4.94
Ti	0.59–0.86	5	0.68	0.48	0.34	0.7	0.63
Al	9.09–10.0	1	9.55	8.05	4.12	6.98	7
Si	23.19–24.73	1	23.97	23.28	10.60	20.43	n/a
				Minor and trace elements (mg/kg)			
Zn	80–377	49	100	60	682	343	65
Cu	81–134	13	99	91	682	301	102
Ge	0.6–1.5	20	1.1	n/a	0.80	n/a	n/a
Ni	13–30	18	21	34	8	9	19
As	4.8–7.3	8	5.7	7.7	12	5	n/a
S	108–392	32	190	110	14206	2190	1297
F	154–463	33	270	n/a	7132	7700	n/a
Rb	9–67	56	23	21	n/a	n/a	n/a
Sr	352–548	14	452	495	1628	1005	n/a
Ba	155–234	11	196	213	150	228	n/a
Cr	22–101	27	55	58	45	48	35
P	611–921	5	758	551	52933	26747	568
V	28–56	10	44	159	89	97	180

Note: Superscripts [a] Geochemical data for the local bedrocks are from Zhao (1991) and Xie et al. (1992); [b] Data for the Y2 lake sediments are from Sun et al. (2001); [c] Geochemical data for the Xihu Lake sediments are from Zhao (1991). CV is coefficient of variation; n/a=not determined.

lake sediments. In Fig. 4, the mean element concentrations in N1 are plotted against those in the local bedrocks. The correlation coefficient between them is 0.99 ($p<0.0001$), which strongly suggests that the local bedrock is the common source of proglacial sediments.

There are statistically significant differences in the mean element concentrations of N1 and Y2, Y4 and Xihu Lake sediments. Samples from Y2 and Y4 have higher concentrations of F, P, Sr, Ba, S, Cu, Zn and Ca, which is attributed to penguin droppings or guanosoil (Sun et al., 2000, 2001; Sun and Xie, 2001). The Xihu Lake sediments have a significantly higher sulfide concentration, probably of biogenic origin (Zhao, 1991). The proglacial sediment sample of N1 was affected neither by penguin droppings nor by biological action, therefore the element concentrations in N1 can be used as natural background in this region for monitoring possible future environmental changes.

In order to explore the possible associations existing between different elements, a Pearson correlation analysis was performed on the 35 subsamples of N1. Here, the examination of the interrelationships of the abundances of elements in the N1 sediment profile attempts to reveal the geological processes affecting the geochemical data, and to interpret the main controlling factors on the element concentrations (Yan et al., 2002). The results (not shown in the paper) show a lack of significant correlations between the concentrations of most elements, except K, Ba and Sr. This may be primarily attributed to the natural effects of grain size distribution and mineral partitioning associated with glacial processes (Jari, 1995; Loring and Asmund, 1996; Tam and Yao, 1998; Klossen, 1999). In order to reduce or eliminate the effect of glacial processes, the ratio of metal to lithogenetic element can be used to normalize geochemical data. Several lithogenetic elements associated with clay minerals (e.g. Al, Cs, Li, Rb, Sc and Co) have been used for the normalization purpose (Allen and Rae, 1987; Aloupi and Angelidis, 2001; Dinescu and Duliu, 2001; Matthai and Birch, 2001). In the present study, a regression of lithogenetic elements mentioned above on clay content was performed and the relative values of correlation coefficients (r) and statistical significance (p) were compared. The results show that only the element Rb is strongly correlated with clay fluctuations in the N1 profile ($r=0.64$, $p<0.001$). This reflects the great capbility of the element Rb to normalize element concentrations in relation to different textures of sediments. Therefore, although there are many lithogenetic elements used as normalizers in previous studies, Rb appears to be better suited for the sediments of the present study area than other elements. Here, we select Rb to normalize the geochemical data of the proglacial sediments. Table 3 gives the correlation matrix for all the element/Rb ratios. As seen from this table, statistically significant correlations ($p<0.001$) are found among the element/Rb ratios. This suggests that these elements, appearing as natural ones, have a common source and are not affected by any significant pollution processes. More importantly, the existence of strong correlations among the element/Rb ratios and the lack of such correlations among absolute element concentrations are important for the evaluation of geochemical data in the Antarctic proglacial area. The element/Rb ratios, characteristic of a particular terrane, can be better used to determine sediment provenance, since elements derived from other sources could significantly change the ratios, result in ratio anomalies and weaken or eliminate the strong correlations.

4.3 Chemical weathering features

Active chemical weathering has long been recognized in periglacial environments (Anderson et al., 2000), though it is generally considered insignificant in terms of the accomplished geomorphic work. Particularly, under the humid condition that occurs around the present ice sheet margin, physical processes, such as frequent diurnal freeze-thaw cycles and high meltwater fluxes in midsummer and glacial grinding, may potentially offset the negative effects of low temperatures, sparse vegetation and poorly developed soils on chemical weathering (Matsuoka, 1995; Anderson et al., 1997; Brown, 2002). Many approaches, including monitoring of solute removal in glacier-derived drainage water, field observation and laboratory analyses of rock and mineral modification and examination of pedogenesis, have been used to study the chemical weathering process in the periglacial region (Caulkett and Ellis-evans, 1997; Anderson et al., 2000; Nezat et al., 2001; Thorn et al., 2001; Brown, 2002). In this paper we focus on the geochemical data of proglacial sediments in order to investigate the glacier-associated chemical weathering. The proglacial sediments in the foreland of the Nelson Ice Cap, as discussed above, are the natural products of local bedrocks, therefore, the element abundances in the sediments can be used to infer the degree of source-area chemical weathering and weathering trends of siliciclastic deposits.

The chemical index of alteration (CIA) proposed by Nesbitt and Yong (1982) is widely used to quantify the degree of source-area chemical weathering process of silicate materials. This index is calculated using molecular proportions:

$$CIA=[Al_2O_3/(Al_2O_3+CaO^*+Na_2O+K_2O)]\times 100$$

where CaO* is the amount of CaO incorporated in the silicate fraction of the deposits.

CIA provides a dimensionless number usually between

Table 3 Pearson correlation matrix for element/Rb ratios in N1

	Zn/Rb	Cu/Rb	Ge/Rb	Ni/Rb	As/Rb	S/Rb	F/Rb	Sr/Rb	Ba/Rb	Cr/Rb	Na/Rb	K/Rb	Ca/Rb	Mg/Rb	Mn/Rb	Ti/Rb	Al/Rb	Si/Rb	P/Rb	V/Rb	Fe/Rb
Zn/Rb	1																				
Cu/Rb	0.92	1																			
Ge/Rb	0.80	0.88	1																		
Ni/Rb	0.80	0.87	0.92	1																	
As/Rb	0.90	0.93	0.86	0.90	1																
S/Rb	0.74	0.74	0.71	0.63	0.77	1															
F/Rb	0.85	0.84	0.71	0.70	0.79	0.66	1														
Sr/Rb	0.92	0.92	0.79	0.82	0.94	0.78	0.90	1													
Ba/Rb	0.93	0.94	0.81	0.82	0.95	0.78	0.91	0.99	1												
Cr/Rb	0.80	0.86	0.86	0.83	0.86	0.77	0.74	0.80	0.81	1											
Na/Rb	0.93	0.94	0.85	0.88	0.95	0.76	0.91	0.98	0.98	0.82	1										
K/Rb	0.92	0.93	0.80	0.81	0.93	0.79	0.92	0.99	0.99	0.80	0.99	1									
Ca/Rb	0.92	0.94	0.88	0.90	0.95	0.78	0.89	0.97	0.97	0.84	0.99	0.97	1								
Mg/Rb	0.90	0.95	0.90	0.95	0.98	0.74	0.83	0.94	0.95	0.85	0.97	0.94	0.98	1							
Mn/Rb	0.86	0.91	0.84	0.89	0.94	0.71	0.80	0.86	0.89	0.82	0.91	0.87	0.92	0.95	1						
Ti/Rb	0.90	0.94	0.86	0.91	0.95	0.75	0.85	0.95	0.95	0.83	0.98	0.96	0.98	0.98	0.91	1					
Al/Rb	0.92	0.96	0.89	0.92	0.98	0.76	0.84	0.97	0.97	0.85	0.98	0.96	0.98	0.99	0.92	0.98	1				
Si/Rb	0.93	0.96	0.88	0.91	0.98	0.77	0.87	0.98	0.98	0.84	0.99	0.97	0.99	0.99	0.93	0.98	1.00	1			
P/Rb	0.86	0.92	0.89	0.96	0.95	0.66	0.79	0.90	0.91	0.81	0.95	0.90	0.96	0.98	0.92	0.96	0.97	0.97	1		
V/Rb	0.85	0.88	0.79	0.82	0.83	0.61	0.90	0.86	0.89	0.72	0.91	0.89	0.91	0.89	0.86	0.88	0.87	0.89	0.87	1	
Fe/Rb	0.92	0.96	0.86	0.91	0.98	0.75	0.85	0.97	0.97	0.86	0.97	0.96	0.98	0.98	0.92	0.98	0.99	0.99	0.96	0.86	1

Note: All the correlations listed in the table are significant at the level of 0.01.

50 and 100. Most fresh igneous rocks yield a value of about 50, except for ultranatic rocks, which have lower values. Shales have a CIA value from 70 to 75, indicating a moderately weathered source. The rocks that are composed entirely of aluminous secondary minerals such as kaolinite and gibbsite have a CIA value of 100. CIA value thus reflects the proportion of primary to secondary minerals in samples (Nesbitt and Yong, 1982; Nesbitt and Markovics, 1997; Young and Nesbitt, 1999). The CIA values for the proglacial sediments in the present study vary between 63 and 70 with an average value of about 66. This value is much higher than that of fresh rocks but less than that of average shales (70–75), indicating a mild chemical weathering process. This suggests that the proglacial sediments near the edge of modern glacier still contain a significant amount of residual feldspar and other alumino-silicates with some chemical weathering.

The nature and extent of chemical weathering undergone by the proglacial sediments can also be evaluated by plotting the bulk compositions (in molar proportions) on triangular diagrams such as A-CN-K and A-CNK-FM plots suggested by Nesbitt et al. (1989, 1992). In the A-CN-K plot (Fig. 5a), the observed weathering trend is almost parallel to the A-CN joint, indicating a loss of plagioclase component (depletion of elements Ca and Na) during the weathering and transport. This may be because plagioclase is more susceptible to weathering and grinding than K-feldspar (Nesbitt and Young, 1984, 1989; Nesbitt et al., 1996). The appearance of mostly unweathered K-feldspar in the sediments is confirmed by the element intercorrelations. As illustrated in Fig. 6, there are strong correlations among K, Sr and Ba concentrations in the proglacial sediments. The correlations between these elements may be attributed to the mineralogical control of K-feldspar as a result of poor chemical weathering process, since K-feldspar is the main carrier for these elements (Zhao and Yan, 1994; Kim et al., 1998). Furthermore, the average chemical composition of drainage meltwater is on the reverse direction of the weathering trend line, since solutes in meltwater represent soluble fractions from chemical weathering.

In the A-CNK-FM plot (Fig. 5b), the trend of the samples that are depleted of Ca, Na, Fe and Mg is considered to be associated with the alteration of both plagioclase and mafic minerals although only to a small extent (Sharma and Rajamani, 2001). This is a typical weathering trend in many basaltic rocks. The ΣFe plus Mg components leached from fresh bedrocks may be partially related to the differences in the hardness of minerals, e.g. mica was found to comminute more readily than K-feldspar (Jari, 1995). Furthermore, the fact that mafic minerals, usually formed under high temperature and pressure, are susceptible to chemical weathering in surface conditions also contributes to the loss of Fe and Mg.

The above results are also in good agreement with the percentage change of element/Ti ratios between a sediment sample and the unweathered local bedrocks. The percentage change of elemental ratios is calculated according to Nesbitt et al. (1980, 1992):

$$\% \text{ change} = 100 \times [(Rs - Rp)/Rp]$$

where Rs and Rp are the ratios of element/Ti in a sample and its parent material, respectively.

Figure 7 plots the percentage changes of major element ratios. It can be seen from this figure that the proglacial

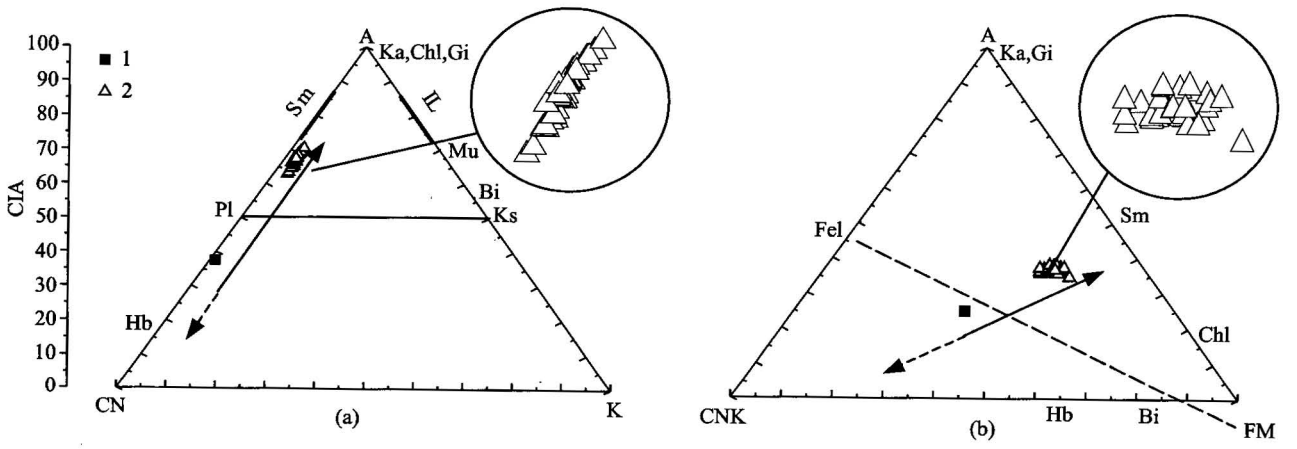

Fig. 5. A-CN-K (a) and A-CNK-FM (b) plots (Nesbitt and Yong, 1989) for proglacial weathering.

1 – Chemical composition in the local bedrocks; 2 — chemical composition in the periglacial sediments. In both plots, the solid-line arrow represents the weathering trend for local fresh bedrocks; the dashed-line arrow represents the reverse extension line of the weathering trend.
In plot (a), A, CN and K represent the molar proportions of Al_2O_3, CaO^*+Na_2O (CaO^* is the amount of CaO in silicate) and K_2O, respectively. Abbreviations: Sm – smectite; Pl – plagioclase; Ks – K-feldspar; Ka – kaolinite; Chl – chlorite; Gi – gibbsite. The trend (shown by the solid-line arrow) is almost parallel to the A-CN joint, indicating little or no loss of K during the chemical weathering. In plot (b), A – Al_2O_3; CNK – $CaO^*+K_2O+Na_2O$; FM – ΣFe+MgO; Fel – feldspar; Hb – hornblende; Bi – biotite.

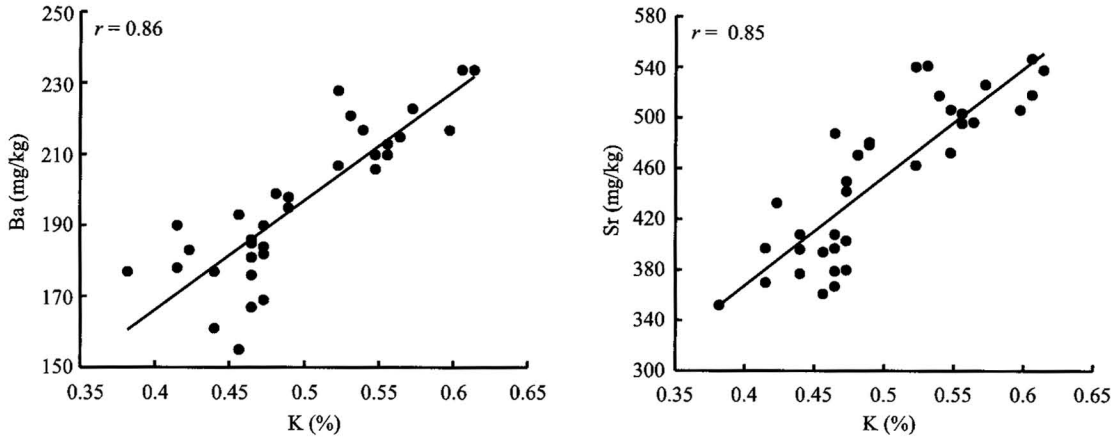

Fig. 6. Relationships between K, Ba and Sr in th eproglacial sediment sample N1. The lines are best fit regression lines.

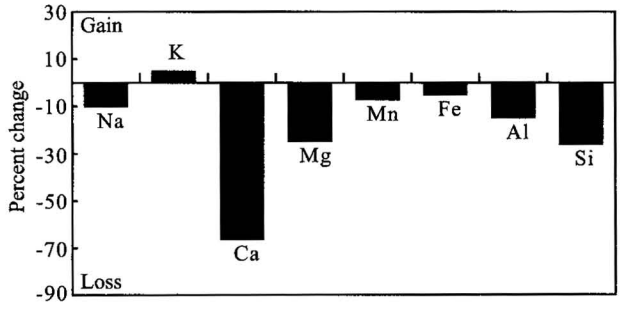

Fig. 7. Percentage changes of the element ratios (with respect to local bedrocks) in the proglacial sediments. The data for the major elements are the averages of 35 subsamples.

sediments have been depleted of most elements as compared to the local bedrocks, except for a slight enrichment of the element K. Of the depleted elements, Ca has the largest loss. This can be explained by its susceptibility to weathering in feldspars. Ca-bearing plagioclase is much more susceptible to weathering than Na-bearing plagioclase and K-feldspar. Consequently, Ca can be released rapidly with the decomposition of Ca-bearing plagioclase (Sawyer, 1986). Furthermore, Na-bearing plagioclase is more susceptible to weathering in comparison to K-feldspar, hence Na is leached preferentially over K. As Nesbitt et al. (1980) have shown, Ca, Na, Fe, Mg and Si are lost to the solutions with progressive weathering, leading to depletion in the residual sediments. The slight enrichment of K may be attributed to the fact that K released from a small quantity of feldspar is almost retained by the clay minerals.

5 Conclusions

This study investigates detailedly the textural and geochemical characteristics of the proglacial sediments near the edge of modern Antarctic glacier. From the results of grain size distributions and element concentrations in these sediments, we can draw the following conclusions:

(1) The grain size distributions of the proglacial sediments are characteristic of glacigenic deposits with a wide-ranging size, extremely poor sorting, positive skewness and broad to medium kurtosis. They are very different from those of aeolian and lacustrine sediments. The grain size distributions of the proglacial sediments are fractal with a dimension of about 2.9, the value of deformed tills.

(2) The absolute element abundances and distributions in the proglacial sediments show irregular variations due to the textural and mineralogical effects associated with glacial processes. Nevertheless, significantly positive correlation ($p<0.001$) can be found among the element/Rb ratios. This finding is significant for the geochemical data processing of the proglacial sediments and the determination of the sediment provenance. The comparison of geochemical data between the proglacial sediments, local bedrocks and the lake sediments indicates that the proglacial sediments are original and have a close genetic relation to the local bedrocks.

(3) Geochemical data of the proglacial sediments can also be used to examine the degree of source-area chemical weathering and weathering trend of siliciclastic deposits. CIA and triangular diagrams such as A-CN-K and A-CNK-FM suggest that the proglacial sediments have undergone mild chemical weathering process of the alteration of Ca- and Na-bearing plagioclases and mafic phase such as mica minerals. This can be explained by the mineral's susceptibility to weathering and the differences in the hardness of minerals resistant to glacial comminution. The percentage changes of element/Ti ratios also show that Ca,

Na, Fe, Mg and Si are lost to the weathering solutions.

Acknowledgements

The work was supported by the National Natural Science Foundation of China (Grant No. 40231002 and 40076032) and the project of Chinese Academy of Sciences (Grant No. KZCX2-303). We sincerely thank the Chinese Polar Administration attached to the National Oceanic Bureau of China for the logical help and support, and are also grateful to Dr. Yuhong Wang for his assistance with the manuscript preparation, and Prof. Yuan Baoyin for providing grain-size data of present Xihu Lake sediments.

Manuscript received May, 21, 2003
accepted Sept. 1, 2003
edited by Zhu Xiling

References

Allen, J.R.L., and Rae, J.Z., 1987. Late Flandrian shoreline oscillations in the Severn estuary: A geomorphological and stratigraphical reconnaissance. *Philosophical Transactions of the Royal Society of London,* Series B, 315: 185–230.

Aloupi, M., and Angelidis, M.O., 2001. Normalization to lithium for the assessment of metal contamination in coastal sediment cores from the Aegean Sea, Greece. *Marine Environmental Research*, 52: 1–12.

Anderson, S.P., Drever, J.I., and Humphrey NF. 1997. Chemical weathering in glacial environment. *Geology*, 25: 399–402.

Anderson, S.P., Drever, J.I., Frost C.D., and Holden P., 2000. Chemical weathering in the foreland of retreating glacier. *Geochim. Cosmochim. Acta*, 64: 1173–1189.

Ballantyne, C.K., 2002. Paraglacial geomorphology. *Quaternary Science Reviews*, 21: 1935–2017

Benn, D.I., and Gemmell, A.M.D., 2002. Fractal dimensions of diamictic particle-size distribution. *Geol. Soc. Am. Bull.*, 114: 528–532.

Brown, G.H., 2002. Glacier meltwater hydrochemistry. *Applied Geochemistry*, 17: 855–883.

Caulkett, A.P., and Ellis-evans, J.C., 1997. Chemistry of streams of Signy Island, maritime Antarctic: sources of major ions. *Antarctic Science*, 9: 3–11.

Church, M., and Ryder, J.M., 1972. Paraglacial sedimentation: a consideration of fluvial processes conditioned by glaciation. *Geol. Soc. Am. Bull.*, 83: 3054–3072.

Dinescu, L.C., and Duliu, O.G., 2001. Heavy metal pollution of some Danube Delta lacustrine sediments studied by neutron activation analysis. *Applied Radiation and Isotopes*, 54: 853–859.

Fischer, U.H., and Hubbard, B., 1999. Subglacial sediment textures: character and evolution at Haut Glacier d'Arolla, Switzerland. *Annals of Glaciology*, 28: 241–246.

Fitzsimons, S.J., 1990. Ice-marginal depositional processes in a polar maritime environment, Vestfold Hills, Antarctica. *Journal of Glaciology*, 36: 279–286.

Fitzsimons, S.J., 1996. Paraglacial redistribution of glacial sediments in the Vestfold Hills, East Antarctica. *Geomorphology*, 15: 93–108.

Folk, R.L., and Ward W.C., 1957. Brazos River bars, a study in the significance of grain size parameters. *J. Sediment. Petrol.*, 27: 3–26.

French, H.M., and Guglielmin M. 1999. Observation on the ice-marginal, periglacial geomorphology of Terra Nova Bay, northern Victoria Land, Antarctica. *Permafrost and Periglacial Processes*, 10: 331–347.

Heiri, O., Lotter, A.F., and Lemcke, G., 2001. Loss on ignition as a method for estimating organic and carbonate content in sediments: reproducibility and comparability of results. *Journal of Paleolimnology*, 25: 101–110.

Hooke, R.L., and Iverson, N.R., 1995. Grain-size distribution in deforming subglacial tills: role of grain fracture. *Geology*, 23: 57–60.

Ingólfsson, O., Hjort, C., Berkman, P.A., Bjorck, S., Colhoum, E., Goodwin, I.D., Hall, B., Hcrakawa, K., Melles, M., Moller, P., and Prentice, M.L., 1998. Antarctica glacial history since the Last Glacial Maximum: an overview of the record on land. *Antarctic Science*, 10: 326–344.

Iverson, N.R., and Hooyer, T.S., 1996. A laboratory study of sediment deformation: stress heterogeneity and grain-size evolution. *Annals of Glaciology*, 22: 167–175.

Jari, M., 1995. Effects of grinding and chemical factors on the generation and composition of the till fine fraction: an experimental study. *Journal of Geochemical Exploration*, 54: 49–62.

Khatwa, A., Hart, J.K., and Payne, A.J., 1999. Grain textural analysis across a range of glacial facies. *Annals of Glaciology*, 28: 111–117.

Kim, G., Yang, H., and Kodama, Y., 1998. Distribution of transition elements in the surface sediments of the Yellow Sea. *Continental Shelf Research*, 18: 1531–1542.

Klossen, R.A., 1999. The application of glacial dispersal models to the interpretation of till geochemistry in Labrador, Canada. *Journal of Geochemical Exploration*, 67: 245–269.

Li Baosheng, David Dian Zhang, Zhou Xingxia, Zhu Feng, Yuan Baoyin, Mu Guijin, Li Sen, Yan Manchun, Jin Heling, Gao Quanzhou, and Sun Wu, 2002. Study of sediments in the Yutian-Hotan Oasis, South Xinjing, China. *Acta Geologica Sinica* (English edition), 76(2): 221–228.

Liu Xiaodong, Sun Li guang, Xie Zhouqing, and Yin Xuebin, 2002. Study on the grain-size fractal features of sediments in Antarctica. *Journal of Glaciology and Geocryology*, 25(4): 394–400 (in Chinese with English abstract).

Liu Shaofeng, Liu Wencan, Dai Shaowu, Huang Siji, and Lu Wuyun, 2001. Thrusting and exhumation processes of a bounding mountain belt: constrains from sediment provenance analysis of the Hefei Basin. *Acta Geologica Sinica* (English edition), 75(2): 144–150.

Loring, D.H., and Asmund, G., 1996. Geochemical factors controlling accumulation of major and trace elements in Greenland coastal and fjord sediments. *Environmental Geology*, 28: 2–11.

Lundqvist, J., Liuieskold, M., and Ostmark, K., 1995. Glacial and periglacial deposits of the Tumbledown Cliffs area, James Ross Island, West Antarctica. *Geomorphology*, 11: 205–214.

Matsuoka, N., 1995. Rock weathering processes and landform development in the Sor Rondane Mountains, Antarctica. *Geomorphology*, 12: 323–339.

Matsuoka, N., and Moriwaki, K., 1992. Frost heave and creep in the Sor Rondane Mountains, Antarctica. *Arctic Alpine Res.*, 24:

271–280.

Matsuoka, N., Moriwaki, K., Iwata, S., and Hirakawa, K., 1990. Ground temperature regimes and their relationship to periglacial processes in the Sor Rondane Mountains, East Antarctica. *Proc. NIPR Symp. Antarct. Geosci.*, 4: 55–66.

Matthai, C., and Birch, G., 2001. Detection of anthropogenic Cu, Pb and Zn in continental shelf sediments off Sydney, Australia—a new approach using normalization with cobalt. *Marine Pollution Bulletin*, 42: 1055–1063.

Nesbitt, H.W., and Markovics, G., 1997. Weathering of granodioritic crust, long-term storage of elements in weathering profiles, and petrogenesis of siliciclastic sediments. *Geochim. Cosmochim. Acta*, 61: 1653–1670.

Nesbitt, H.W., and Wilson, R.E., 1992. Recent chemical weathering of basalts. *Am. J. Sci.*, 292: 740–777.

Nesbitt, H.W., and Young, G.M., 1982. Early Proterozoic climate and plate motions inferred from major element chemistry of lutites. *Nature*, 299: 715–717.

Nesbitt, H.W., and Young, G.M., 1984. Predication of some weathering trends of plutonic and volcanic rocks based on thermodynamic and kinetic considerations. *Geochim. Cosmochim. Acta*, 48: 1523–1534.

Nesbitt, H.W., and Young, G.M., 1989. Formation and diagenesis of weathering profiles. *J. Geol.*, 97: 129–147.

Nesbitt, H.W., Markovics, G., and Price, R.C., 1980. Chemical processes affecting alkalis and alkaline earths during continental weathering. *Geochim. Cosmochim. Acta*, 44: 1659–1666.

Nesbitt, H.W., Young, G.M., Mclennan, S.M., and Keays, R.R., 1996. Effects of chemical and sorting on the petrogenesis of siliciclastic sediments, with implications for provenance studies. *J. Geol.*, 104: 525–542.

Nezat, C.A., Lyons, W.B., and Welch, K.A., 2001. Chemical weathering in streams of a polar desert (Talor Valley, Antarctica). *Geol. Soc. Am. Bull.*, 113: 1401–1408.

Rin, J.W., Qin, D.H., Petit, J.R., Jouzel, J., Wang, W.T., Liu, C., Wang, X.T., Qian, S.L., and Wang, X.X., 1995. Glaciological studies on Nelson Island, South-Shetland Island, Antarctica. *J. Glaciology*, 41: 408–412.

Sawyer, E.W., 1986. The influence of source rock type, chemical weathering and sorting on the geochemistry of clastic sediments from the Quetico metasedimentary belt, superior provenance, Canada. *Chemical Geology*, 55: 77–95.

Sharma, A., and Rajamani, V., 2000. Major element, REE, and other trace element behavior in Amphibolite weathering under semiarid conditions in southern India. *J. Geology*, 108: 487–496.

Sharma, A., and Rajamani, V., 2001. Weathering of charnockites and sediment production in the catchment area of the Cauvery River, southern India. *Sedimentary Geology*, 143: 169–184.

Sun Liguang, Xie Zhouqin and Zhao Junlin, 2000. A 3,000-year record of penguin populations. *Nature*, 407: 858.

Sun Liguang, Xie Zhouqin and Zhao Junlin, 2001. The sediments of lake on the Ardley Island, Antarctica: identification of penguin-dropping soil. *Chinese Journal of Polar Science*, 12: 1–8.

Sun Liguang and Xie Zhouqin, 2001. Relics: penguin population programs. *Science Progress*, 84: 31–44.

Tam, N.F.Y., and Yao, M.W.Y., 1998. Normalisation and heavy mental contamination in mangrove sediments. *The Science of the Total Environment*, 216: 33–39.

Thorn, C.E., Darmody, R.G., Dixon, J.C., and Schlyter, P., 2001. The chemical weathering regime of Karkervagge arctic-alpline Sweden. *Geomorphology*, 41: 37–52.

Xie Youyu, Guan Ping., Yang Shaojin, Chen Binru and Yang Yiming, 1992. Geochemistry of sediments and environment in Xihu Lake of Great Wall Station of China, Antarctica. *Sci. China* (B), 35: 758–768.

Yan Quanren, Gao Shanlin, Wang Zongqi, Li Jijiang, Xiao Wenjiao, Hou Quanlin, Yan Zhen and Chen Haihong, 2002. Geochemical constraints of sediments provenance, depositional environment and tectonic setting of the Songliao Prototype Basin. *Acta Geologica Sinica* (English edition), 76(4): 455–462.

Young, G.M., and Nesbitt, H.W., 1999. Paleoclimatology and provenance of the glaciogenic Gowganda Formation (Paleoproterozoic), Ontario, Canada: a chemostratigraphic approach. *Geol. Soc. Am. Bull.*, 111: 264–274.

Zhao Junlin, 1991. *The Characteristics of the Modern Environmental Geochemistry and Natural Environmental Evolution in the Region of Antarctic Great Wall Station.* Beijing: Science Press, 1–99 (in Chinese with English abstract).

Zhao Yiyang and Yan Mingcai, 1994. *Geochemistry of Sediments of the China Shelf Seas.* Beijing: Science Press, 37–49 (in Chinese).

Zheng Xiangshen, Sang Haiqing, Qiu Ji, Liu Jiaqi, Lee Jong IK, and Kim Hyeoncheol, 2000. New discovery of the Early Cretaceous volcanic rocks on the Barton Peninsula, King George Island, Antarctica and its geological significance. *Acta Geologica Sinica* (English edition), 74(2): 176–182.